The effect of area averaging on the approximated profile of the Hα spectral line

Marcela Bodnárová,[1] Dominik Utz,[2] and Ján Rybák[1]

[1]*Astronomical Institute, Slovak Academy of Sciences, Tatranská Lomnica, SK 059 60, Slovak Republic;* mbodnarova@astro.sk

[2]*IGAM/Institute of Physics, University of Graz, Universitätsplatz 5, A–8010 Graz, Austria;* dominik.utz@uni-graz.at

Abstract. The Hα line is massively used as a diagnostics of the chromosphere. Often one needs to average the line profile over some area to increase the signal to noise ratio. Thus it is important to understand how derived parameters vary with changing approximations. In this study we investigate the effect of spatial averaging of a selected area on the temporal variations of the width, the intensity and the Dopplershift of the Hα spectral line profile. The approximated profile was deduced from co-temporal observations in five points throughout the Hα line profile obtained by the tunable Lyot filter installed on the Dutch Open Telescope. We found variations of the intensity and the Doppler velocities, which were independent of the size of the area used for the computation of the area averaged Hα spectral line profile.

1. Introduction

The solar coronal plasma is an ionized gas which is mainly structured by the ubiquitous presence of magnetic flux tubes and open magnetic field lines. These structures demonstrate sizes over very large scales, right down to the current observational limit, and are maintained at temperatures of several million Kelvin. The heating processes that generate, and sustain the hot corona have so far defied quantitative understanding, despite efforts spanning more than half a century (Kuperus et al. 1981; Gomez 1990; Zirker 1993; Ofman 2005; Klimchuk 2006; Taroyan & Erdélyi 2009; Mathioudakis et al. 2013). Efforts to establish the causes of solar atmospheric heating (of the chromosphere and the corona) have produced a number of theories, of which two classes are most promising.

The first class of theories holds for current dissipation, following reconnection events occurring throughout the atmosphere in the form of micro-flare and nano-flare activity (Parker 1988; Priest & Schrijver 1999; Fujimoto et al. 2011). These energetic jets are the direct consequences of magnetic reconnection and their observational evidence has been reported in the chromosphere (Shibata et al. 2007; Katsukawa et al. 2007; De Pontieu et al. 2007).

The second class of theories predicts that the heating is produced by magnetohydrodynamic (MHD) waves (Alfvén 1947; Osterbrock 1961; Ionson 1978), most likely caused and driven by dynamic processes in the lower atmosphere and then traveling upwards (Roberts 2000). In uniform plasma, there are three distinct types of MHD waves:

slow and fast magneto-acoustic waves, and Alfvén waves. The first two types of waves have an acoustic character modified by the magnetic field, whereas the Alfvén waves exist purely because of the presence of a magnetic field (Erdélyi & Fedun 2007). These waves, guided by the magnetic fields, may transport the energy of powerful photospheric motions into the corona leading to plasma heating (Mathioudakis et al. 2013).

Fast and slow mode magneto-acoustic waves cause compression and rarefaction of the plasma as they propagate. These waves can cause both intensity variations and Doppler shifts (Mathioudakis et al. 2013). Alfvén waves are incompressible, and capable of penetrating through the solar atmosphere without being reflected or refracted (Ofman 2002). Their propagation through the atmosphere is not associated with density changes seen as periodic variations of intensities and line-of-sight velocities (Jess et al. 2009; Mathioudakis et al. 2013). In the case of a slanted magnetic fluxtube Alfvén waves could manifest as periodic variations of non-thermal broadening of a spectral line (Erdélyi & Fedun 2007) and should thus be observed as full-width half-maximum oscillations (Zaqarashvili 2003).

We use the algorithm developed by Koza et al. (2013) in a study of spectral characteristics of an area averaged profile of the Hα spectral line. Essentially, we focus on temporal variations of the line width, the intensity, and the Doppler velocity of the Hα profile for various sizes of a spatial averaging window applied to the data.

2. Observation and Data Processing

We used data sets of speckle-reconstructed images of the quiet solar chromosphere taken in Hα: in the core of the line profile (λ_c = 656,3 nm) and in four points in the wings of the line profile ($\lambda = \lambda_c \pm 0.035$ nm and $\lambda = \lambda_c \pm 0.07$ nm, respectively) recorded by the Dutch Open Telescope (DOT: Rutten et al. 2004). The time sequence was collected on 19 October 2005, at 09:55 − 11:05 UT, under good seeing conditions from a network region close to the disk center (location N00/W09, $\mu = 0.983$). All five data sets consist of 71 speckle-reconstructed images obtained by the Keller - von der L*ü*he two channel speckle-reconstruction (Keller & von der Luhe 1992) with $r_0 \geq 7$ cm and with a cadence of 60 s. These images have been reconstructed from bursts of 20 images taken with rate of 6 images per second. All speckle-reconstructed images have a field of view (FOV) of 79×58 arcsec^2, with a spatial sampling of 0.071 arcsec per pixel.

The coarse five-point sampling of the Hα line profile enables us to construct $1112 \times 818 \times 71$ instantaneous five-point profiles of the Hα spectral line, one profile for each pixel of the field of view (1112×818 pixel^2) in each of the 71 time steps (separated by 60 s). For the purposes of our study we computed average profiles of the Hα spectral line for a selected sub-field (region of interest; ROI) of the full FOV in order to eliminate the effect of anomalous pixels. We employed the algorithm developed by Koza et al. (2013) to fit the five-wavelength samples of the proxy profiles by a 4th order polynomial function. For this area-averaged profile we derived the four spectral parameters: the intensity in the line center I_c, the width of the profile w_p, the Doppler velocity v_c (dopplershift of the line center), and the Doppler velocity v_p (dopplershift of the line profile). More detailed information about the algorithm (testing and obtained results) can be found in Koza et al. (2013, 2014).

The values of I_c and v_c represent the fit minimum and its dopplershift, respectively. The width of the profile w_p is the wavelength separation I_p of the two fit flanks at half of

the intensity range between the fit minimum and the average intensity of the endpoint intensities at ±0.07 nm defined as

$$I_p = \frac{\langle I_{-0.7}, I_{+0.7} \rangle + I_c}{2}$$

where I_c is the intensity in the line center and $\langle I_{-0.7}, I_{+0.7} \rangle$ is the mean of the two intensities measured at the wavelength points of $\lambda = \lambda_c - 0.07$ nm and $\lambda = \lambda_c + 0.07$ nm.

The definition of the Doppler velocity v_p is based on the method originally introduced by Scherrer et al. (1995) to calculate velocities for the observations of the MDI instrument on the SOHO spacecraft. According to this method a ratio of differences of the four filtergrams F_1 through F_4 is calculated

$$\begin{aligned} \alpha &= (F_1 + F_2 - F_3 - F_4)/(F_1 - F_3) \\ \text{if} \quad & (F_1 + F_2 - F_3 - F_4) > 0 \quad \text{or} \\ \alpha &= (F_1 + F_2 - F_3 - F_4)/(F_4 - F_2) \\ \text{if} \quad & (F_1 + F_2 - F_3 - F_4) \leq 0 \end{aligned}$$

where F_1 is represented by the intensity measured in the profile of the Hα line at $\lambda = \lambda_c - 0.07$ nm, F_2 is the intensity measured at $\lambda = \lambda_c - 0.35$ nm, F_3 is the intensity measured at $\lambda = \lambda_c + 0.35$ nm and F_4 is the intensity measured at $\lambda = \lambda_c + 0.07$ nm. Based on the obtained value of α, the Doppler velocity v_p is estimated using a look-up table constructed based on simulations using parametrized solar line profiles (Koza et al. 2013).

3. Analysis and Results

From the total FOV (79 ×58 arcsec^2) of DOT we selected a small sub-field (ROI) for which we applied the area averaging before the computation of the spectral characteristics of the Hα line profile. This ROI is centered at a prominent network region (identified via the intensity enhancements as seen in co-spatial and co-temporal Ca II images). Moreover it was selected due to the high activity and occurrence of prominent structures (bright jet-like mottles) in the H$\alpha(\lambda_c)$ images during the observational sequence. Thus, this ROI is appropriate to study the influence of the area averaging process for a set of averaging windows of various sizes (squares with dimensions between 5×5 pixels^2 and 81×81 pixels^2). In addition the possible effect of the occurrence of single bright mottles during the temporal evolution of the four studied spectral characteristics of the Hα line profile is investigated. Figure 1 shows the selected ROI in G-band, Ca II H and Hα, together with the illustration of different sizes of the selection window. During the duration of the observation the selected ROI (applied for all different sizes and all three types of data) contained at times a variety of structures of evolving shapes at different locations. Thus making it impossible to select an area (large or small) which would represent the same kind of behavior during the whole duration of the observation. The proposed set of averaging windows was chosen in order to test the effect of this variability of structures on the deduced mean spectral characteristics of the area averaged Hα line profile.

We obtained the spectral characteristics of the area averaged Hα line profile for six areas of various sizes. In Figure 2 (top left) we present a comparison of the obtained

values of the central intensity I_c, for area averaging done over squares from 5×5 pixels^2 to 81×81 pixels^2. The presented evolution of I_c exhibits prominent peaks during the second half of the observation. The position of these peaks does not change depending on the size of the particular averaging window. We performed a similar comparison for the other three spectral characteristics: v_c, v_p and w_p, also shown on Figure 2. For v_c (top right) and v_p (bottom left) we obtained similar results as in the case of I_c. Four prominent peaks during the second half of the observation could be related to similar peaks in I_c and can be an indication of a possible periodicity. The results for w_p (bottom right) show, that this parameter exhibits random-like variations within a small range of values, indistinguishable from noise.

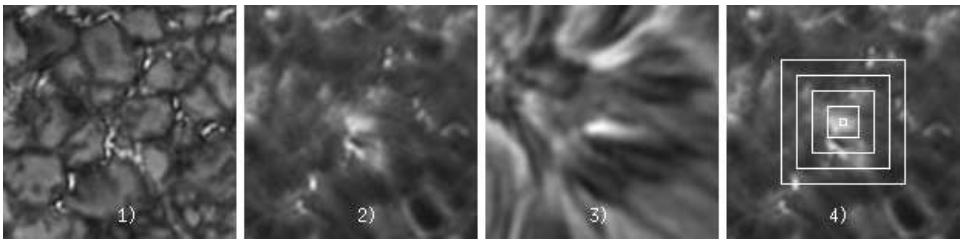

Figure 1. A subfield of the FOV of DOT, centered at the selected ROI - from left to right: 1) in G-band; 2) in Ca II H; 3) in Hα; and 4) the sizes and locations of the averaging window in relation to the selected network region.

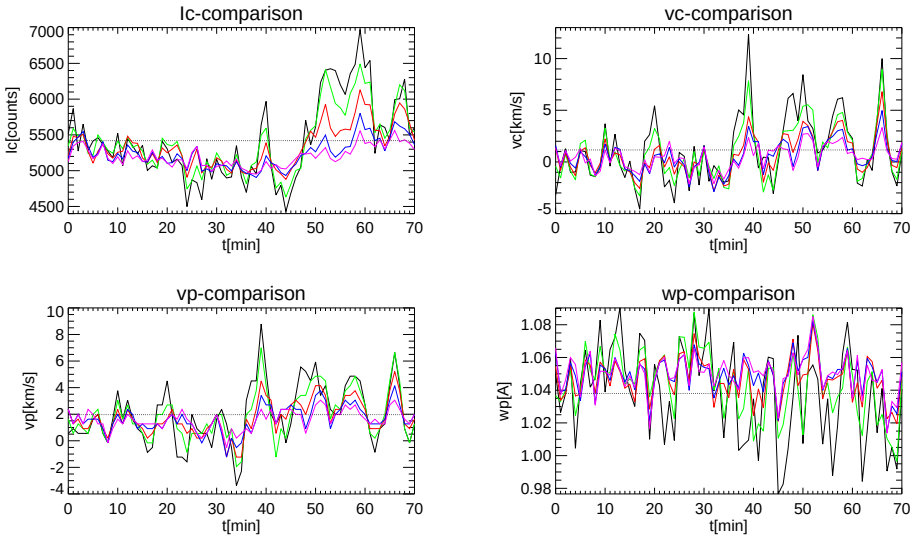

Figure 2. The variations of the area averaged I_c, v_c, v_p and w_p for areas of different sizes for the whole duration of the observation: 5×5 (black), 21×21 (green), 41×41 (red), 61×61 (blue) and 81×81 (magenta) pixels^2. The horizontal line indicates the mean value for the smallest averaging window. (The colored figure can be found in the electronic version)

4. Conclusions

We studied the temporal evolution of four spectral characteristics (I_c, w_p, v_c and v_p) of of the area averaged Hα spectral line profile for different sizes of a selection window in the range from 0.355×0.355 arcsec^2 to 5.751×5.751 arcsec^2 derived from the DOT instrument observations. Our findings suggest that while averaging over areas of larger sizes (> 41 arcsecs window side length) may cause a decrease in the observed peaks of the temporal evolution of the Hα spectral characteristics, it has to be done over much larger areas in order to obliterate these peaks. Thus a signal originating in a small subfield of the selection window (e. g. a small network element) can become even more prominent for the area averaged profile, even for larger averaging window, as the noise level will be strongly suppressed due to the averaging. Also, a survey of single pixel profiles of the Hα spectral line support our finding that, the centered network element might be the source of the observed variations. Our analysis provides a suitable tool for the selection of the suitable selection window size to study the observed variations in detail. Moreover, three of the four studied parameters (I_c, v_c and v_p) indicate the occurrence of significant changes in the selected area during the second half of the observation and suggest that whatever might have caused this change has a periodic nature.

Acknowledgments. The Technology Foundation STW in the Netherlands financially supported the development and construction of the DOT and follow-up technical developments. The DOT has been built by instrumentation groups of Utrecht University and Delft University (DEMO) and several firms with specialized tasks. The DOT is located at Observatorio del Roque de los Muchachos (ORM) of Instituto de Astrofísica de Canarias (IAC). DOT observations on 19 October 2005 have been funded by the OPTICON Trans-national Access Programme and by the ESMN-European Solar Magnetic Network - both programs of the EU FP6. The authors thank P. Sütterlin for the DOT observations, R. Rutten for the data reduction and J. Koza for algorithm development. This work was supported by the Slovak Research and Development Agency under the contract No. APVV-0816-11.We acknowledge support by the project VEGA 2/0004/16. This article was created by the realisation of the project ITMS No.26220120009, based on the supporting operational Research and development program financed from the European Regional Development Fund.

References

Alfvén, H. 1947, MNRAS, 107, 211
De Pontieu, B., McIntosh, S. W., Carlsson, M., Hansteen, V. H., Tarbell, T. D., Schrijver, C. J., Title, A. M., Shine, R. A., Tsuneta, S., Katsukawa, Y., Ichimoto, K., Suematsu, Y., Shimizu, T., & Nagata, S. 2007, Science, 318, 1574
Erdélyi, R., & Fedun, V. 2007, Science, 318, 1572
Fujimoto, M., Shinohara, I., & Kojima, H. 2011, Space Sci.Rev., 160, 123
Gomez, D. O. 1990, , 14, 131
Ionson, J. A. 1978, ApJ, 226, 650
Jess, D. B., Mathioudakis, M., Erdélyi, R., Crockett, P. J., Keenan, F. P., & Christian, D. J. 2009, Science, 323, 1582. 0903.3546
Katsukawa, Y., Berger, T. E., Ichimoto, K., Lites, B. W., Nagata, S., Shimizu, T., Shine, R. A., Suematsu, Y., Tarbell, T. D., Title, A. M., & Tsuneta, S. 2007, Science, 318, 1594
Keller, C. U., & von der Luhe, O. 1992, A&A, 261, 321
Klimchuk, J. A. 2006, Solar Phys., 234, 41. astro-ph/0511841
Koza, J., Rybák, J., Gömöry, P., & Kučera, A. 2014, Contributions of the Astronomical Observatory Skalnate Pleso, 44, 43
Koza, J., Sütterlin, P., Gömöry, P., Rybák, J., & Kučera, A. 2013, Contributions of the Astronomical Observatory Skalnate Pleso, 43, 5. 1304.4027
Kuperus, M., Ionson, J. A., & Spicer, D. S. 1981, ARA&A, 19, 7
Mathioudakis, M., Jess, D. B., & Erdélyi, R. 2013, Space Sci.Rev., 175, 1. 1210.3625
Ofman, L. 2002, ApJ, 568, L135
— 2005, Space Sci.Rev., 120, 67
Osterbrock, D. E. 1961, ApJ, 134, 347
Parker, E. N. 1988, ApJ, 330, 474
Priest, E. R., & Schrijver, C. J. 1999, Solar Phys., 190, 1
Roberts, B. 2000, Solar Phys., 193, 139
Rutten, R. J., Hammerschlag, R. H., Bettonvil, F. C. M., Sütterlin, P., & de Wijn, A. G. 2004, A&A, 413, 1183
Scherrer, P. H., Bogart, R. S., Bush, R. I., Hoeksema, J. T., Kosovichev, A. G., Schou, J., Rosenberg, W., Springer, L., Tarbell, T. D., Title, A., Wolfson, C. J., Zayer, I., & MDI Engineering Team 1995, Solar Phys., 162, 129
Shibata, K., Nakamura, T., Matsumoto, T., Otsuji, K., Okamoto, T. J., Nishizuka, N., Kawate, T., Watanabe, H., Nagata, S., UeNo, S., Kitai, R., Nozawa, S., Tsuneta, S., Suematsu, Y., Ichimoto, K., Shimizu, T., Katsukawa, Y., Tarbell, T. D., Berger, T. E., Lites, B. W., Shine, R. A., & Title, A. M. 2007, Science, 318, 1591. 0810.3974
Sütterlin, P., Hammerschlag, R. H., Bettonvil, F. C. M., Rutten, R. J., Skomorovsky, V. I., & Domyshev, G. N. 2001, in Advanced Solar Polarimetry – Theory, Observation, and Instrumentation, edited by M. Sigwarth, vol. 236 of ASP Conf. Ser., 431
Taroyan, Y., & Erdélyi, R. 2009, Space Sci.Rev., 149, 229
Zaqarashvili, T. V. 2003, A&A, 399, L15. astro-ph/0301316
Zirker, J. B. 1993, Solar Phys., 148, 43